Institute of Electronics, Information, and Communication Engineers

PAPER *Special Issue on Radar Technology*

Detection of Objects Buried in Sandy Ground by a Synthetic Aperture FM-CW Radar

Yoshio YAMAGUCHI† *and* **Masakazu SENGOKU**†, *Members*

SUMMARY An FM-CW radar system for the detection of objects buried in sandy ground is explored and is applied to a field measurement. The key factors for underground FM-CW radar performance are the center frequency and bandwidth determining the depth at which the radar can detect targets and the resolution in the range direction. In order for FM-CW radar sounding, two ridged horn antennas are employed in the system, which are operative in the frequency range of 250–1000 MHz. The impedance matching to the ground is optimized by measuring the echo strength from a fixed target as a function of the spacing interval between the antenna aperture and the ground surface. It is shown that the radar with an output power of 18 dBm could detect a metallic plate (30×100 cm) and a pipe (10 cmϕ) buried at the depth of 1.2 m. Also the synthetic aperture technique together with an averaging and subtracting method produced fine image in shallow region up to 100 cm in the sandy ground.

key words: *radio applications, FM-CW radar, SAR, underground radar*

1. Introduction

Ground penetrating radar has been attracting interest in recent years for the purpose of detecting pipes (communication cables, water and gas pipes, electricity cables), broken sewers, historical remains, archaeological exploration, etc. [1]–[9]. Ground penetrating radar can roughly be classified into three types: pulsed-radar, continuous wave radar, and coded radar. Most of the ground penetrating radar are pulse-based radars. The pulse radar itself has a long historical background, and many theoretical and experimental investigations have been carried out heretofore [10]–[12]. However, as far as deep sounding is concerned, it is very difficult, regardless of radar type, because the wave attenuation in the underground restricts the sounding capabilities. For the detection of deep target, it is necessary to use low frequencies (for example, lower than 100 MHz). The lower the frequencies, the deeper the radar can detect target. But, for high resolution imaging, it is necessary to use the frequency bandwidth as wide as possible (for example, more than 1000 MHz bandwidth). Various efforts including STC technique [10], modulation technique [8], and signal processing [3], [12] have been carried out to overcome the difficulty in deep sounding problem.

This paper describes the synthetic aperture FM-CW radar system and presents the detection result of objects buried in a sandy ground. To the author's knowledge, there is very little successful synthetic aperture FM-CW radar applications to underground targets [13], [14]. The purpose of the paper is to show the possibility of synthetic aperture FM-CW radar for underground application. The FM-CW radar utilizes a wideband and continuous frequency signal for the detection. The flat frequency characteristics is the most important factor for the FM-CW radar. This leads to several advantages and disadvantages as follows,

Advantages:

(1) High sensitivity—If the system frequency characteristics is flat, maximum signal to noise (S/N) ratio is guaranteed, because the time-domain beat signal in an FM-CW system, produced at a mixer, is essentially an output of matched filter. Therefore, the S/N ratio is always maximized.
(2) Low power—This is the consequence of (1).
(3) Simple equipments.
(4) Easy to build up a system.
(5) The range accuracy can be adjusted easily by a signal processing software.

Disadvantages:

(6) Difficulty to realize a practical radar antenna. In general, it is extremely difficult to realize high gain practical antenna with flat frequency characteristics such as input impedance, radiation pattern, etc., in such a wide and low frequency region.
(7) Spurious beat signal may come out due to non-flatness of frequency characteristics.
(8) Difficulty in wideband impedance matching between antenna and ground.
(9) Impossible to employ STC technique (time-gated method) in pulse radar system to limit undesired reflected signal such as ground surface echo.

In order to overcome the disadvantages (6) and (8), two ridged horn antennas operative in the 250–1000 MHz were explored in this work. The impedance matching (8) was optimized by checking the echo strength, by varying the spacing interval between the antenna aperture and the ground surface. Then an explored FM-CW radar system was applied to detect a metallic plate of 30×100 cm and a pipe of 10 cmϕ in

Manuscript received April 23, 1993.
Manuscript revised June 10, 1993.
† The authors are with the Faculty of Engineering, Niigata University, Niigata-shi, 950-21 Japan.

NII-Electronic Library Service

Institute of Electronics, Information, and Communication Engineers

a sandy ground. The field measurement revealed that the radar system could detect and image these targets at the depth of 120 cm with low output power (68 mW). The result is displayed in two dimensional radar image showing a potential ability of FM-CW radar in detection operations.

Section 2 explains the principle of synthetic aperture FM-CW radar, Sect. 3 describes the antenna and system, followed by the experimental and signal processing results in Sect. 4.

2. Principle of Synthetic Aperture FM-CW Radar

In this section, a brief description of basic principles necessary for introducing the synthetic aperture technique, based on the Fresnel hologram transformation approach, is given.

The FM-CW radar basically measures the distance between a radar antenna and an object by the beat frequency of the transmitted and reflected signal from the object. The transmitting signal is usually swept linearly from $f_0-\Delta f/2$ to $f_0+\Delta f/2$ where f_0 is the center frequency. Figure 1 shows the relation of frequency and time in the FM-CW radar. If a point object whose reflection coefficient function is represented by

$$g=g(x_0, z_0),$$

$$(x_0, z_0):\ \text{coordinate of the object} \tag{1}$$

is located at a distance r from the transmitting antenna in a medium of permittivity ε_r, the reflected signal from the target arrives at the radar with a time delay by $\tau(\tau=2r/c\sqrt{\varepsilon_r},\ c=3\times10^8\ \text{m/s})$. This reflected signal and the instantaneous transmitted signal is mixed at a mixer, producing a beat signal whose frequency is given by

$$f_b=\tau\frac{\Delta f}{\Delta t}r=\frac{2\sqrt{\varepsilon_r}}{c}\frac{\Delta f}{\Delta t}r \tag{2}$$

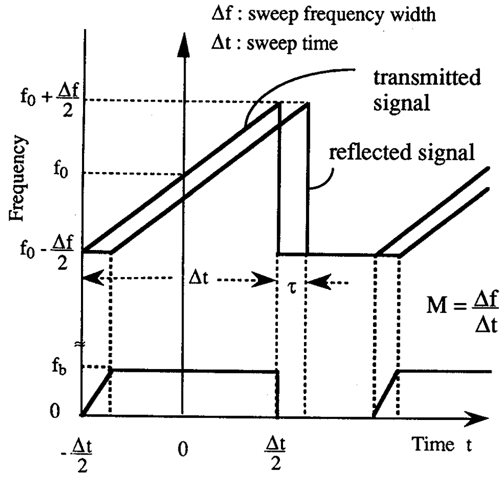

Fig. 1 Relation between frequency and time in FM-CW radar.

where,

Δf: sweep frequency width,

Δt: sweep time.

Therefore the distance r is determined by obtaining f_b. This is the well-known principle of the FM-CW radar. In our system, f_b is determined via Fourier transform of the time domain beat signal. The Fourier transform with respect to time $(-\Delta t/2\leqq t\leqq\Delta t/2)$ for the positive frequency domain results in[15]

$$U(f)=Bg\exp(-j2\pi f_0\tau)\frac{\sin[\pi(f-f_b)\Delta t]}{\pi(f-f_b)\Delta t} \tag{3}$$

with B being the amplitude. It should be noted that Eq. (3) contains the phase term due to the time delay τ.

The FM-CW radar scene is obtained by antenna scanning. The real aperture image formulation is essentially based on Eq. (3) without the phase term [16]. Now, the synthetic aperture technique which is to be applied to the real aperture FM-CW radar is explained as follows. Let's assume that a reflection point exists at a distance r in the Fresnel region as shown in Fig. 2. The time delay τ can be approximated as,

$$\tau=\frac{2\sqrt{\varepsilon_r}}{c}r\approx\frac{2\sqrt{\varepsilon_r}}{c}\left[z_0+\frac{(x-x_0)^2}{2z_0}\right] \tag{4}$$

Under this assumption, the Fourier transformed beat spectrum (3) becomes a function of space variable only, and can be written as

$$U(x,z)=Bf(z-z_0)g(x_0,z_0)h(x-x_0,z_0) \tag{5}$$

where,

$$f(z-z_0)=\frac{\sin[\alpha(z-z_0)]}{\alpha(z-z_0)}=\text{Sinc}[\alpha(z-z_0)] \tag{6}$$

is the range function in the z direction with $\alpha=2\pi\sqrt{\varepsilon_r}/c\cdot\Delta f$, and

$$h(x-x_0,z_0)=\exp\left[-j\frac{4\pi\sqrt{\varepsilon_r}f_0}{c}\left\{z_0+\frac{(x-x_0)^2}{2z_0}\right\}\right] \tag{7}$$

is the phase function with respect to the propagation

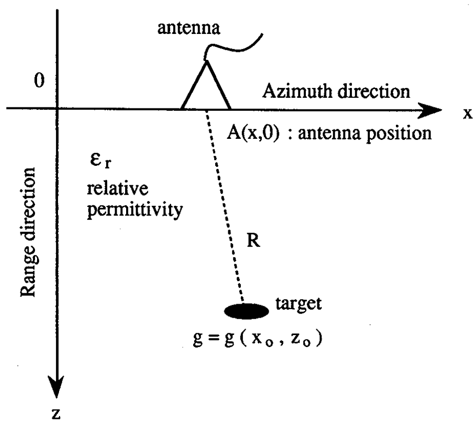

Fig. 2 Location of radar and target in a medium with ε_r.

NII-Electronic Library Service

Institute of Electronics, Information, and Communication Engineers

path.

If the target possesses a two-dimensional areal distributions both in the azimuth direction, x_0, and in the range direction, z_0, then the beat spectrum (5) should be modified as,

$$U(x, z)=B\int_0^\infty\int_{-\infty}^\infty f(z-z_0)\,g(x_0, z_0)\,h(x-x_0, z_0)\cdot dx_0\,dz_0 \qquad (8)$$

One can see that this expression of the convolution integral form and that it is equivalent to a Fresnel approximation to the Kirchhoff-Fresnel diffraction integral equation. Therefore, we may consider it as one kind of hologram.

At $z \approx z_0$, and if the frequency width is wide enough, i.e., $\alpha \gg 1$, which is in our case, the range function $f(z-z_0)$ can be approximated as

$$f(z-z_0)=\begin{cases}1, & z=z_0\\ 0, & z\neq z_0\end{cases} \qquad (9)$$

which leads to

$$U(x, z_0)=B\int_{-\infty}^\infty g(x_0, z_0)\,h(x_0-x, z_0)\,dx_0 \qquad (10)$$

The object distribution function $g(x_0, z_0)$ can be obtained by an inverse convolution integral after multiplying the complex conjugated function h^* by U.

$$g(x_0, z_0)=\int_{-\frac{L}{2}}^{\frac{L}{2}} U(x, z_0)\,h^*(x_0-x, z_0)\,dx \qquad (11)$$

L in Eq. (11) is the antenna-scan width in the scanning direction, and symbol * denotes complex conjugation. This equation is the basis for the synthetic aperture FM-CW radar principle.

The object reflection distribution function g can be found via Fourier transformation

$$g(x_0, z_0)=FT^{-1}[FT(U)\cdot FT(h^*)] \qquad (12)$$

where

FT: Fourier Transform,

FT^{-1}: Inverse Fourier Transform.

3. Antennas and Radar System

As mentioned before, the flat frequency characteristics is the most important for the FM-CW radar system. The radar antenna plays an important role for the system. Since low and wideband frequency antenna is required, for example, operative in 100-1000 MHz, we have chosen a ridged horn as a radar antenna because of its compactness with respect to the wavelength and its wideband frequency characteristics. The detailed explanation of the ridged waveguide and horn is given in Refs.[17] and [18], respectively. We have decided to operate it from 250 MHz so that the antenna can be used in an actual detection operation. Otherwise the antenna becomes impractically large if the lowest operating frequency is chosen less than 200 MHz. Figure 3 shows the return loss of an explored antenna placed at 30 cm above a sandy ground. Nominally, 10 dB return loss is obtained throughout the 380-850 MHz frequency range. Two antennas were designed, one is for transmission and the other is for reception. The maximal dimension size is $60\times48\times116.5$ cm, and the aperture is 60×48 cm.

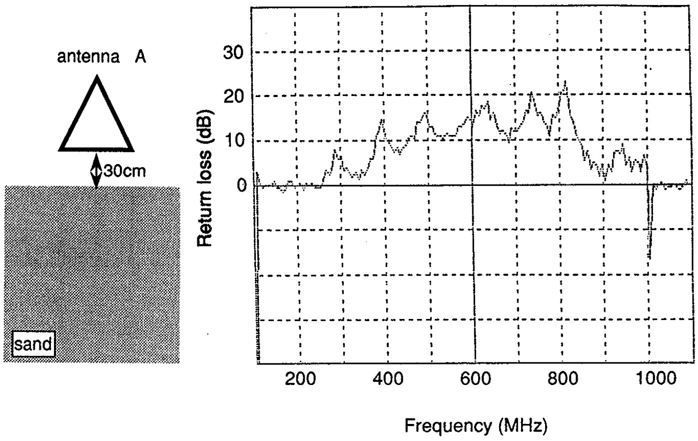

Fig. 3 Return loss of a ridged horn antenna.

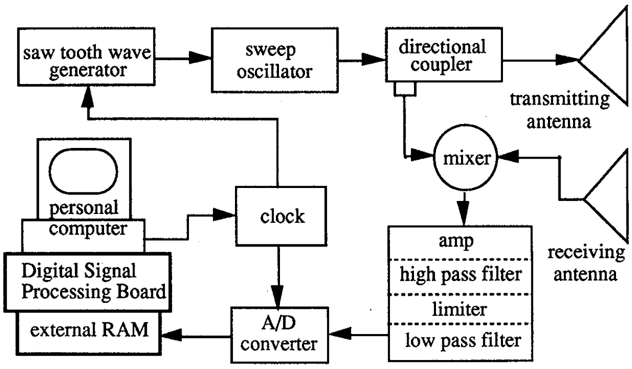

Fig. 4 Block diagram of FM-CW radar.

Table 1 FM-CW radar specifications.

RF generator power	18 dBm
Frequency	250-1000 MHz
Antenna	Rectangular ridged horn
Polarization	Linear
Sweep time	5.2 ms
Range Accuracy	2 cm in the air
Controller	16-bit personal computer

Using the ridged horn antennas, an FM-CW radar system was designed as shown in Fig. 4. The specification of the radar is listed in Table 1. A saw tooth generator triggers a sweep oscillator, and the generated FM-CW signal goes through a directional coupler where most of the signal is transmitted via the

NII-Electronic Library Service

Institute of Electronics, Information, and Communication Engineers

transmitting antenna. The remaining part of the signal is derived directly to a mixer where the reflected signal from a target is combined and the square detection is carried out. After amplifying and filtering the squared signal, it is possible to obtain a desired beat signal whose frequency is proportional to the target distance r. The Fourier transform of this time domain signal is executed at a personal computer using FFT algorithm. Finally, a real aperture FM-CW response (beat spectrum) is displayed on a CRT display. Successful scanning of antenna produces a real aperture radar scene which is a basis for synthetic aperture image.

4. Field Experiment and Signal Processing

4.1 Matching

At first, an impedance matching to the ground was examined. Impedance matching at a single frequency could be easily performed by a quarter-wavelength plate as used in the transmission line theory. However, since the FM-CW radar utilizes a wideband signal, it is extremely difficult to match the impedance between the antenna and a ground surface over the entire frequency region. In addition, the radiated field in this problem is close to so-called "near field" where the far field (i.e., TEM) approximation is not valid. Therefore, we took a magnitude of spectrum due to a fixed target as a measure of matching factor and measured it by varying the spacing between the antenna aperture and the ground surface. Figure 5(a) shows the experimental scheme. Both the transmitting and the receiving radar antennas were moved at 2 cm intervals from 10 up to 50 cm above the surface. At each interval, it is possible to extract the strength due to a single target (in this case, the target is a metallic plate of 30 cm × 100 cm). The detected strength is shown in Fig. 5(b) as a function of spacing interval. It is seen that the spacing of 30 cm provides the maximum detection strength. At this spacing, the impedance matching seems to be optimized for the entire operating frequency bandwidth. The detected strength varies as much as 16 dB. Thus, the spacing between antenna and ground surface is found to be an important factor for detection operations. It should be noted that the optimum spacing interval may change at a different experimental situation, i.e., it is dependent on frequency, antenna size, and permittivity of medium. Although similar theoretical results at a single frequency are presented in Refs.[19] and [20], a further theoretical investigation on the optimum spacing will be needed, taking account of wideband signal, medium property, etc.

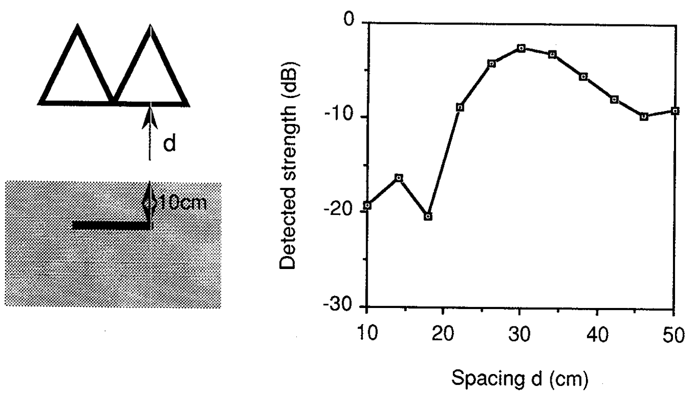

(a) Experimental scheme. (b) Detected strength.

Fig. 5 Detection strength as a function of spacing.

4.2 Detection Result and Signal Processing

Using the spacing of 30 cm, a detection measurement was carried out. The first target is the same metallic plate used in the matching. It was buried in a sandy ground at the depth of 30 cm. The reason why we have chosen sandy ground is that our university is located where almost all ground is sand. The antenna was

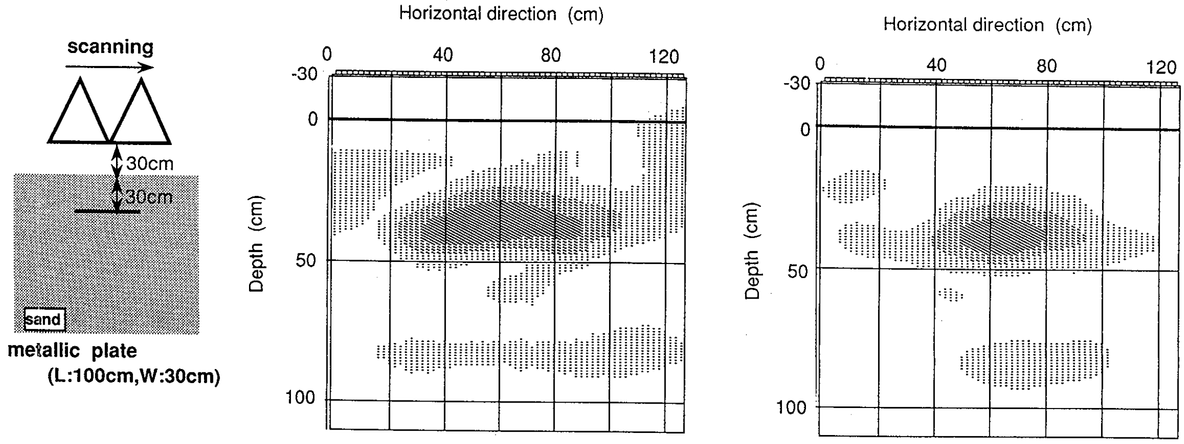

(a) Experimental scheme. (b) Real aperture image. (c) Synthetic aperture image.

Fig. 6 Detection result of a metallic plate at 30 cm deep.

NII-Electronic Library Service

Institute of Electronics, Information, and Communication Engineers

scanned over the surface as indicated in Fig. 6(a). The scanned length was 128 cm with an incremental length of 2 cm which produced 64 raw data. Figure 6(b) shows the magnitude of the spectrum (real aperture detection image) of the plate by a quasi-gray scale, with black indicating strong reflection. Nine uniformly spaced gray-scale levels have been used to cover the magnitude range in the Fourier transformed domain. The horizontal direction corresponds to the scanned length, while the vertical axis corresponds to the radar detection range. This radar range is calibrated by an estimated permittivity of 4.62, which is derived after the measurement taking account of free space propagation path. Thus the vertical axis represents the actual depth. (Since we know the actual depth of target, it is possible to estimate the permittivity of the sand by comparing the radar detection range). It is seen that the target is well detected by the radar, although there are some reflections due to medium inhomogeneities.

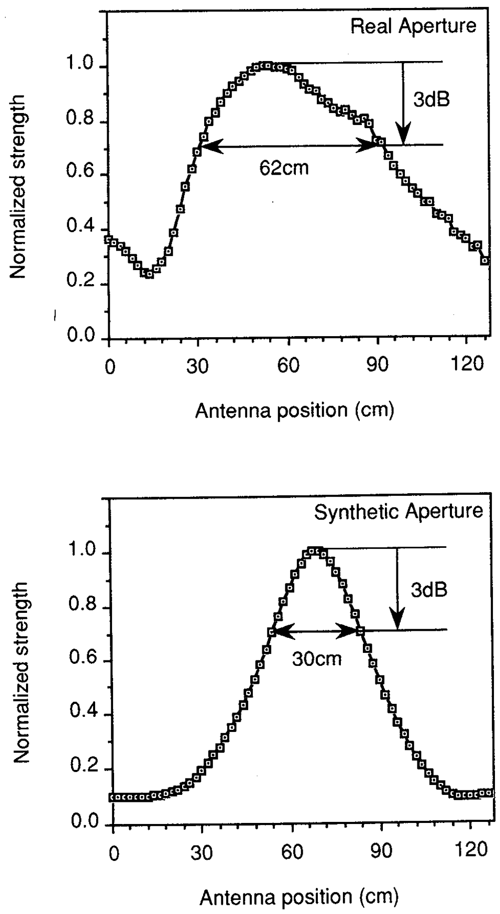

Fig. 7 Resolution by synthetic aperture processing.

Synthetic aperture processing yields the target image of Fig. 6(c). The resolution in the horizontal direction is improved by this technique. And clutter component is suppressed slightly. To confirm quantitatively the effect of synthetic aperture technique, we examined the resolution in the scanning direction by the radar detection profile as shown in Fig. 7. Both normalized real aperture and synthetic aperture profile are compared to show the difference of the beam width due to the same target. The beam width defined here is the 3 dB width as shown in Fig. 7. The target depth is 30 cm. It is seen that the width of 62 cm in the real aperture is reduced to 30 cm in the synthetic aperture profile. Therefore the resolution is increased by 2 times. In the free space, the synthetic aperture width is 28 cm.

Similar profiles were calculated, resulting in 34, 30, and 48 cm in the synthetic aperture width for the depth of 60, 90 and 120 cm, respectively. As the depth increases, the effect of synthetic aperture processing fades out. However, the detection profile becomes smooth by the synthetic aperture processing. This

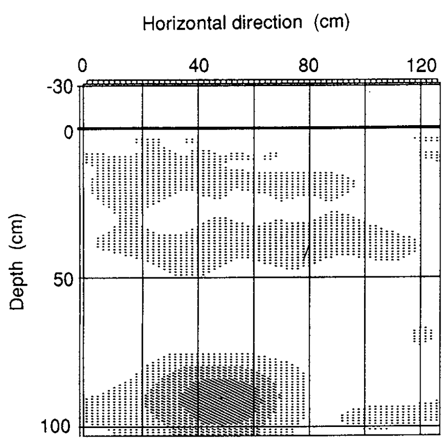

(a) 90 cm deep.

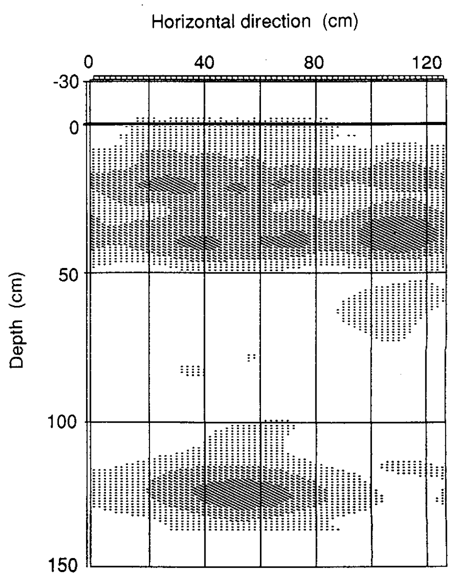

(b) 120 cm deep.

Fig. 8 Synthetic aperture image of a metallic plate (30 cm × 100 cm).

NII-Electronic Library Service

Institute of Electronics, Information, and Communication Engineers

phenomenon seems to be caused by the sandy medium whose electrical properties are lossy, dispersive and inhomogeneous. As far as the sandy ground under the measurement is concerned, the synthetic aperture technique is effective for shallow region up to approximately 100 cm deep.

The synthetic aperture images of the metallic plate at different depth are illustrated in Figs. 8(a) and (b). It is seen that the explored FM-CW radar could detect the target clearly at 120 cm deep. The small difference in the detected depth of Fig. 8 is due to an estimated permittivity error which is dependent on each experiment, i.e., the sand above the target was dug and was put back in each detection measurement. Strictly speaking, the medium above the target differs slightly case by case. On the other hand, the same estimated permittivity 4.62 is used throughout the calculation.

In order to suppress clutter in synthetic aperture image in Fig. 8, we examined a method of averaging and subtracting. The algorithm of method is:

1) average the value of column data at a certain depth in a synthetic aperture image,
2) transform the original data at that depth into a new one after subtracting the averaged value from the

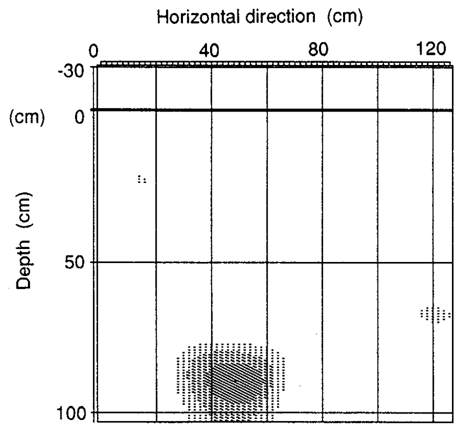

(a) 90 cm deep.

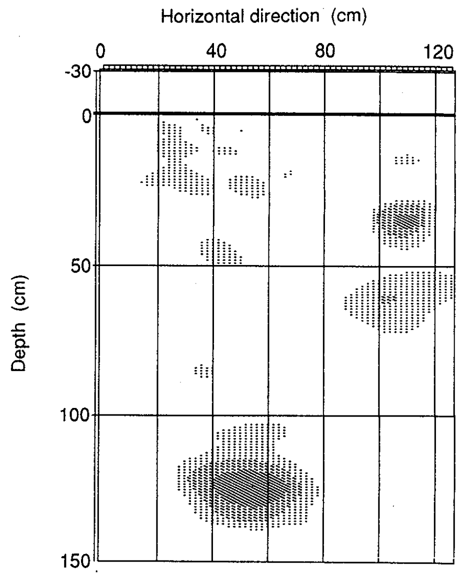

(b) 120 cm deep.

Fig. 9 Processed image of a metallic plate by a method of averaging and subtracting.

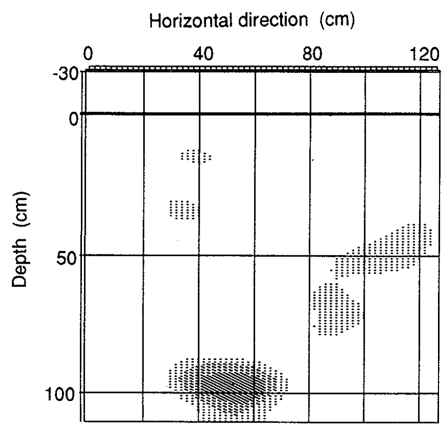

(a) 90 cm deep.

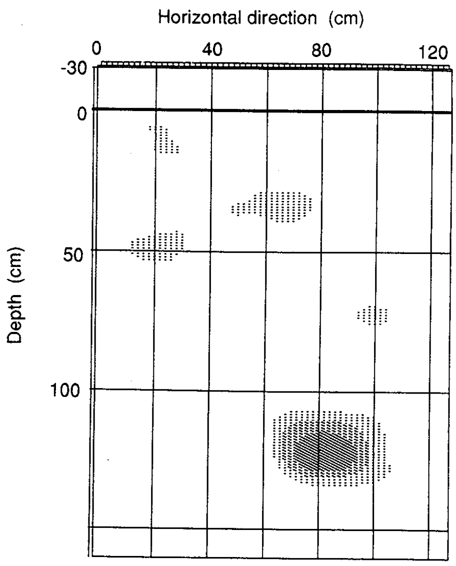

(b) 120 cm deep.

Fig. 10 Processed image of a pipe (10 cmϕ) by a method of averaging and subtracting.

NII-Electronic Library Service

Institute of Electronics, Information, and Communication Engineers

original one [16],
3) re-normalize the new data.

The resultant image of a metallic plate is shown in Fig. 9. The corresponding image for a metallic pipe of 10 cmϕ is shown in Fig. 10(a)-(b). This method renders the target image clear, suppressing noise, although it seems to be effective only for a horizontally homogeneous medium.

5. Conclusion

An FM-CW radar system was applied to detect objects buried in a sandy ground. Two ridged horn radar antennas operative in the frequency range of 250-1000 MHz were designed for underground detection. The impedance matching to the ground was optimized by measuring the detection strength from a fixed target as a function of the spacing interval between the antenna aperture and the ground surface. The fact that the detected strength varied as much as 16 dB in the experiment indicates importance of the spacing interval between antenna and surface. It was possible to detect a metallic plate (30×100 cm) and a pipe (10 cmϕ) buried at the depth of 1.2 m with an output power of 18 dBm. The synthetic aperture processing together with an averaging and subtracting method produced fine smooth target images, suppressing noise for the sandy ground. For a deep target more than 100 cm deep, the effect of synthetic aperture technique faded out. The depth boundary, where the synthetic aperture processing is effective, is dependent on the medium property under measurement.

It still be needed to investigate how to sound deep target by FM-CW radar. One method is to use high power radar and the other is to use more efficient antennas. These points will be treated in the near future.

Acknowledgement

Authors are grateful to Dr. Kikuta T., Nishino M., and Tsunasaki M. of Osaka Gas R & D Center for providing the experimental equipment. Special thanks are extended to the students, Masahiro TSURUGI and Yutaka WATANABE, at Niigata University for assisting the measurement. This work in part is supported by Grant-in-Aid for Scientific Research on Priority Areas, Ministry of Education, Japan.

References

[1] Arai, I. and Suzuki, T., "Advance on underground radars," *Trans. IEICE*, vol. E74, no. 2, pp. 289-294, Feb. 1991.

[2] Osumi, N. and Ueno, K., "Microwave holographic image of underground objects," *IEEE Trans. Antennas & Propag.*, vol. AP-33, no. 2, pp. 152-159, Feb. 1985.

[3] Michiguchi, Y., Hiramoto, K., Nishi, M., Ootaki, T. and Okada, M., "Advanced subsurface radar system for imaging buried pipes," *IEEE Trans. Geosci. & Remote Sensing*, vol. 26, no. 6, pp. 733-740, Nov. 1988.

[4] Arai, I. and Suzuki, T., "Synthetic aperture for subsurface radars," in *Proc. of ISAP'85* (Kyoto, Japan), pp. 655-658, Aug. 1985.

[5] Suzuki, T., Arai, I. and Xiao, D., "Coded pulse underground radar," *IEICE Technical Report*, SANE87-1, Jan. 1987.

[6] Nagamune, M. and Tezuka, K., "Coded pulse compression underground radar," *1989 Nat. Conv. Rec. IEICE*, B-149.

[7] Tezuka, K. and Nagamune, A., "A highly sensitive cross bore-hole radar by M-seq. signal processing," in *Proc. of the 2nd Workshop on Subsurface Electromagnetic Measurements*, pp. 117-122, Dec. 1992.

[8] Arai, I., Tomizawa, Y., and Suzuki, T., "Pulse compression subsurface radar using delay correlator," in *Proc. of the 2nd Workshop on Subsurface Electromagnetic Measurements*, pp. 111-116, Dec. 1992.

[9] Yamaguchi, Y. and Sengoku, M., "Detection of buried objects by an FM-CW radar," in *Proc. of the 2nd Workshop on Subsurface Electromagnetic Measurements*, pp. 103-110, Dec. 1992.

[10] Skolnik, M. I., *Introduction to Radar Systems*, second edition, McGraw-Hill, KOGAKUSYA, Tokyo, 1980.

[11] Wehner, D. R., *High Resolution Radar*, Artech House, Massachusetts, 1987.

[12] Sekine, M., *Radar Signal Processing Techniques*, IEICE, Tokyo, 1991.

[13] Dennis, P. and Gibbs, S. E., "Solid-state linear FM/CW radar systems-their promise and their problems," *Proc. IEEE MTT Symp.*, 1974, pp. 340-342, 1974.

[14] Iizuka, K. and Freundofer, A., "Detection of nonmetallic buried objects by a step frequency radar," *Proc. of the IEEE*, vol. 71, no. 2, pp. 276-279, Feb. 1983.

[15] Yamaguchi, Y., Mitsumoto, M., Kawakami, A., Sengoku, M. and Abe, T., "Detection of objects by synthetic aperture FM-CW radar," *Trans. IEICE*, vol. J74-B-II, no. 7, pp. 413-420, Jul. 1991.

[16] Yamaguchi, Y., Maruyama, Y., Kawakami, A., Sengoku, M. and Abe, T., "Detection of buried objects in wet snowpack by an FM-CW radar," *IEEE Trans. Geosci. & Remote Sensing*, vol. 29, no. 2, pp. 201-208, Mar. 1991.

[17] Cohn, S. B., "Properties of the ridge waveguide," *Proc. of IRE*, vol. 35, pp. 783-789, Aug. 1947.

[18] Walton, K. L. and Sudberg, V. C., "Broadband ridged horn design," *Microwave J.*, vol. 7, pp. 96-101, Mar. 1964.

[19] Smith, G. L., "Directive properties of antennas for transmission into a material halfspace," *IEEE Trans. Antennas & Propag.*, vol. AP-32, no. 3, pp. 232-246, Mar. 1984.

[20] Ishizuka, Y., Yamaguchi, Y. and Sengoku, M., "Field distribution in snowpack by boundary element analysis," *IEICE Technical Report*, AP92-99, Nov. 1992.

NII-Electronic Library Service

Institute of Electronics, Information, and Communication Engineers

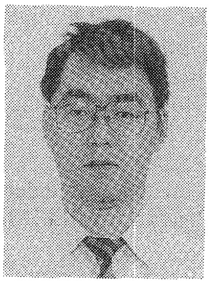

Yoshio Yamaguchi was born in Niigata, Japan, on March 12, 1954. He received the B.E. degree in electronics engineering from Niigata University in 1976, and the M.E. and Dr.Eng. degrees from Tokyo Institute Technology, Tokyo, Japan, in 1978 and 1983, respectively. In 1978, he joined the Faculty of Engineering, Niigata University, where he is now an Associate Professor. From 1988 to 1989, he was a Research Associate at the University of Illinois at Chicago. His interests are in the field of propagation characteristics of electromagnetic waves in lossy medium, radar polarimetry, microwave remote sensing and imaging. Dr. Yamaguchi is a member of IEEE, and the Japan Society for Snow Engineering.

Masakazu Sengoku was born in Nagano Prefecture, Japan, on October 18, 1944. He received the B.E. degree in electrical engineering from Niigata University, Japan, in 1967 and the M.E. and Ph.D. degrees from Hokkaido University in 1969 and 1972, respectively. In 1972, he joined the staff at Hokkaido University as a Research Associate. In 1978, he was an Associate Professor at Niigata University, where he is presently a Professor. During 1986-1987, he was a Visiting Scholar at the University of California, Berkeley, and at the University of Illinois, Chicago. His research interests include transmission of information, network theory, and graph theory. He is a recipient of the best paper award of IEICE in 1992. Dr. Sengoku is a member of the Japan Society for Industrial and Applied Mathematics, and IEEE.

NII-Electronic Library Service